Viscous Properties and Dynamic Electrooptical Performance in Twisted Nematic Displays of Several Liquid Crystal Classes

Paul R. Gerber and M. Schadt
F. Hoffmann-La Roche & Co. Limited Company, 4002 Basel, Switzerland

Z. Naturforsch. **37a**, 179–185 (1982); received February 3, 1982

For the 65th aniversary of Professor Walter Boguth

The temperature dependence of the rotational viscosities of several physically markedly different binary mixtures belonging to ten different liquid crystal classes is measured. An attempt is made to correlate the results with class-specific structural properties such as hydrogenated rings, molecular polarity and structure of flexible side-chains. It is show that the measured small-scale dynamic properties of twist cells compare well with approximative theoretical calculations and experimientially determined class-specific material parameters. For the switching times corresponding to large-scale twist deformations heuristic approximations lead to satisfactory results.

1. Introduction

Viscous properties of nematic liquid crystals have been determined only rarely in the past, the determination of the whole 5-component viscosity tensor being a tedious task indeed [1, 2, 3]. There are, however, some viscosity coefficients which can be determined with an acceptable experimental effort like the flow-aligned shear viscosity η_s or the rotational viscosity γ_1. η_s is characteristic for the flow-aligned state of the nematic and can be determined in conventional viscometers. Due to its easy determination the shear viscosity has conventionally been used to characterize the overall viscous properties of commercial nematics. It has, however, the disadvantage of being a fairly complicated combination of simpler viscosity coefficients and depends in certain cases even on ratios of elastic constants. Therefore, the relation between η_s and the dynamic properties of most electro-optical applications of liquid crystals is rather indirect. Contrary to η_s the rotational viscosity γ_1 plays probably a major role in the response behaviour of nematics in practical applications. However, its determination requires an increased experimental effort [4, 5]. It is the purpose of the present work to extend our investigations of the dielectric, optical and elastic material properties in a series of binary mixtures [6] that belong to different liquid crystal classes by measurements of γ_1 and η_s as well as by experimental and theoretical investigations of the dynamics of twisted-nematic displays. Besides, first qualitative attempts to relate γ_1 with molecular properties are made.

2. Substances and Experimental

On the one hand the substances chosen for the experiments belong to a series of binary mixtures

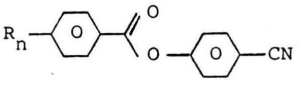
= En ,

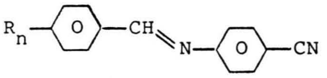
= Sn ,

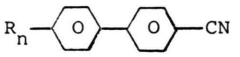
= K3n,

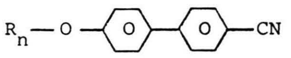
= M3n,

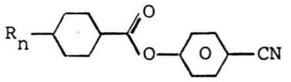
= PEn,

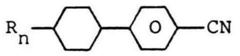
= PCn,

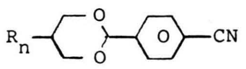
= PDn,

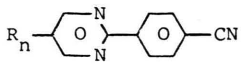
= Pn ,

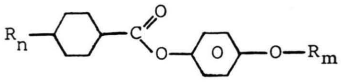
= nECm ,

$R_n = C_nH_{2n+1}$.

Reprint requests to Dr. M. Schadt, F. Hoffmann-La Roche & Co., Limited Company, CH-4002 Basel.

0340-4811 / 82 / 0200-0179 $ 01.30/0. — Please order a reprint rather than making your own copy.

from different liquid crystal classes. Each of the binaries is composed of a pentyl and a hexyl component. On the other hand a second series of binaries was investigated, each composed of one and the same component which was doped with different components belonging to various chemical classes. The structures used were MBBA and the ones drawn above.

The composition of the binary mixtures — binaries were chosen mainly to enlarge the mesomorphic ranges — is given in Table 1. They are denominated after the substance classes. Also given in Table 1 are the clearing temperatures $\mathrm{U_c}$ of the mixtures. More information on possible smectic mesophases and estimates of melting temperatures can be found in [6].

The shear flow viscosity η_s which is characteristic for the flow-aligned state of nematics was measured in a Brookfield rotating cone viscometer (LVT).

The determination of γ_1 required measurements of the reorientation kinetics of the nematic director in a changing magnetic field as described recently in [7]. Besides, the magnetic susceptibility anisotropy $\Delta\chi$ had to be known. $\Delta\chi$ was determined at a single temperature by comparing the threshold voltage and threshold magnetic field of the Freedericks-transitions. For other temperatures $\Delta\chi$ was estimated by assuming proportionality between $\Delta\chi(T)$ and the refractive index anisotropy $\Delta n(T)$ taken from [6].

The electro-optical measurements were performed in conventional 90° twist cells made with SiO_x-evaporated, 10 μm-spaced substrates which induce nearly tilt-free wall alignment. The response times measured in cells with slightly different spacings ($\pm 10\%$) were corrected to a thickness of 10 μm by utilizing the proportionality between response time and square of the reciprocal cell thickness. The response of the transmission of the cell when placed between parallel polarizers using normally incident light of 546 nm was recorded on a transient recorder.

3. Viscosities

3.1. Measurements

Figure 1 shows the logarithm of γ_1 and η_s (in Poises) versus the inverse absolute temperature for the class specific mixtures 1 to 9. Some of the shear-viscosity data have been published before [3], but for the sake of comparison they are included. The general features of the ln γ_1 vs T^{-1}-curves are (i) a rather steep, slightly upwards bended increase for decreasing temperature and (ii) an enhanced decrease of γ_1 near the clearing point, a behaviour which is characteristic for the presence of a virtual critical point. The main aspects distinguishing the graphs $\gamma_1(T^{-1})$ of the substances in Fig. 1 are the values of γ_1 at a fixed temperature (far from all critical regions) which differ by a factor ~ 4.5 among different LC-classes and the respective slopes T_{a,γ_1} taken at a fixed reduced temperature $T_R = 0.92\, T_c$. These slopes have the meaning of an activation temperature (or activation energy when multiplied by the Boltzman constant) in an Arrhenius-type interpretation. Another quantity showing significant variation among different LC-classes is the ratio γ_1/η_s taken at constant reduced

Table 1. Composition, clearing temperature, rotational viscosity γ_1 at 25 °C of several class-specific binary mixtures. Also shown are the ratios γ_1/η_s and the activation temperatures T_{a,γ_1} and T_{a,η_s} determined at a reduced temperature $T_R = 0.92\, T_c(\mathrm{K})$ from $T_{a,\gamma_1} \equiv \mathrm{d} \ln \gamma_1[\mathrm{Poise}]/\mathrm{d}T^{-1}[\mathrm{k}^{-1}]$. Values for MBBA are taken from [7]. The last two columns show the susceptibility anisotropy $\Delta\chi$ and the temperature $T_{\Delta\chi}$ at which this value was measured.

Mixture	Composition 60 Mol%, 40 Mol%	T_c [°C]	γ_1 (25 °C) [Poise]	γ_1/η_s at T_R	$T_{a,\gamma_1}(T_R)$ [kK]	$T_{a,\eta_s}(T_R)$ [kK]	$\Delta\chi$ [10^{-8}]	$T_{\Delta\chi}$
MBBA	pure	44.3	0.89	3.05	6.63	6.43		
E	(E7, E5)	56.2	4.10	5.21	6.48	5.50	10.6	35.0
S	(S7, S5)	70.7	3.60	4.57	5.36	4.63	12.0	25.0
K	(K7, K5)	39.4	1.02	4.35	5.58	4.89	10.0	25.0
M	(M7, M5)	71.6	3.71	3.97	5.71	4.79	10.5	50.0
PE	(PE7, PE5)	80.2	2.69	6.36	4.43	3.96	3.7	45.0
PC	(PC7, PC5)	55.6	1.20	5.64	4.92	4.16	3.7	39.0
PD	(PD7, PD5)	49.8	1.34	3.10	5.59	4.99	2.5	40.0
P	(P7, P5)	51.0	2.01	4.62	5.64	4.99	12.9	39.4
EC	(3EC4, 3EC2)	74.1	1.39	6.21	4.33	2.72	5.3	40.0

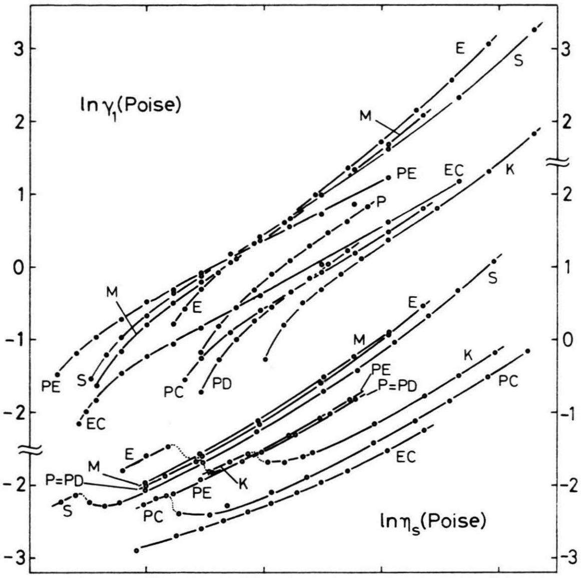

Fig. 1. Logarithm of the measured rotational viscosity γ_1 (upper graphs) and of the measured flow aligned viscosity η_s (lower graphs) versus inverse absolute temperature for the class-specific mixtures of Table 1. Note the different zero-levels for ln γ_1 and ln η_s.

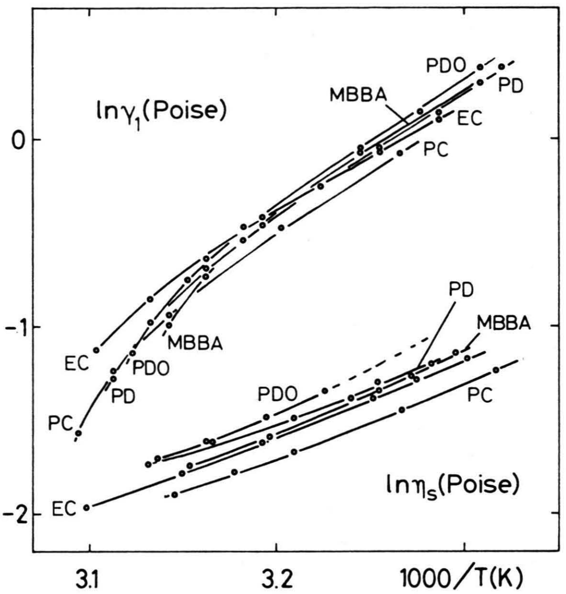

Fig. 2. Measurements of ln γ_1 and ln η_s versus inverse temperature for mixtures containing P7. The labels on the graph correspond with the mixture denomination of Table 2.

temperature T_R. These ratios depicted in Table 1 are found to vary between 3 and 6.

A second group of binary mixtures investigated are composed of (P7, X) = (60%, 40%), where X denotes a component belonging to an other liquid crystal class.

The compositions of these mixtures are listed in Table 2. Figure 2 shows measurements of the viscosities of these mixtures versus reciprocal temperature. Because of the rather narrow mesomorphic ranges of (P7, X) comparisons of γ_1 between different binaries were made not at 25 °C as in Table 1 but at 32 °C (c.f. Table 2). Their activation temperatures T_{a,γ_1} and viscosity ratios γ_1/η_s were determined at $T_R = 0.94\,T_c$ (Table 2). In order to see special effects occurring upon mixing different LC-classes we have in addition calculated the following two differences in the γ_1-values (at 32 °C = constant): (i) the difference between the γ_1-values of (P7, X) and P = (P7, P5) divided by the molar ratio of component X which is $c = 0.4$, and (ii) the difference between the values of the class-specific mixtures X and P. For ideal mixing behaviour one might expect equality of these two quantities, which are shown in Table 2.

Table 2. Composition, clearing temperature and γ_1-values at 32 °C of several mixtures containing P7. The values of γ_1/η_s and of T_{a,μ_1} are taken at a reduced temperature $T_R = 0.94$. The last columns show the change $\delta\gamma_1$ in γ_1 per molar concentration c of added component X and the difference $\Delta\gamma_1$ between the γ_1-values of mixtures P and X (composition as shown in Table 1) taken at 32 °C.

Mixture	Composition 60/40 [Mol.%]	T_c [°C]	γ_1 (32 °C) [Poise]	γ_1/η_s	$T_{a,\mu_1}(T_R)$ [kK]	$\Delta\chi$ 10^{-8}	$T_{\Delta\chi}$	$\frac{\delta\gamma_1}{c}$	$\Delta\gamma_1$
P	(P7, P5)	51.0	1.32	4.39	5.73	12.9	39.4	0	0
P/PD	(P7, PD5)	49.8	1.10	3.82	6.24	7.7	39.5	− 0.55	− 0.48
P/PDO	(P7, 5PDO3)	48.8	1.17	3.60	6.72	8.9	40.0	− 0.38	—
P/PC	(P7, PC5)	50.3	0.99	4.14	6.53	7.2	39.0	− 0.83	− 0.49
P/MBBA	(P7, MBBA)	47.0	1.11	4.06	6.44	13.5	36.0	− 0.53	− 0.77
P/EC	(P7, 5EC3)	51.5	1.05	3.78	5.58	8.2	40.0	− 0.68	− 0.34

3.2. Discussion

A first characteristic feature of γ_1 is its enhanced decrease for temperatures approaching the clearing temperature T_c. This feature may be understood by the almost second order nature of the clearing transition in nematics. However, our systems are not well suited for a quantitative study of critical properties such as the determination of critical exponents because extrapolations to a rather uncertain fictive second order transition temperature would be necessary.

To get some insight into possible correlations between γ_1 and molecular structure it is interesting to compare the measurments of γ_1 (25 °C) in Table 1 among structurally similar molecules like the ester linked E, PE and EC, or the directly linked ring systems K, M and PC as well as the molecules PD and P comprising heterocyclic rings. The measurements indicate that strongly positive dielectric substances [6], like the aromatic cyano esters E or the cyano Shiff'bases S (compared for instance with the nonpolar Schiff'base MBBA) exhibit large rotational viscosities. The same trend was found for γ_1 of the positive dielectric hydrogenated esters PE compared with the nonpolar esters EC (Table 2) which both comprise the same rigid molecular core. In the case of the esters and S which — due to the respective ester and Schiff'base linkages — are relatively elongated molecules, γ_1 may also be affected by their rather long rigid cores which appear likely to increase γ_1 also. Comparing γ_1 of the molecules P and PD, which both contain directly linked heterocyclic rings, with the directly linked non-heterocyclic compounds K and PC in Table 2 gives some indication of a γ_1-raising effect of heterocyclic rings. Possibly this enhancement in γ_1 may have its origin in the stronger polarity of the heterocyclic molecules which have larger dielectric anisotropies [6].

A comparison between γ_1 of K and PC in Table 1 shows the surprising result that the aromatic binary K exhibits a lower rotational viscosity than the structurally similar but hydrogenated PCs, whereas the order is reversed when considering the respective shear viscosities (Figure 1). An analogous behaviour was found for γ_1 and η_s in the upper temperature range of the aromatic esters E compared with the hydrogenated PEs (Figure 1). Thus, disregarding the effect of hydrogenation on the temperature dependence, hydrogenation of benzene rings appears to have little influence on γ_1 in the compounds investigated.

Comparing γ_1 of the alkyl biphenyl K with the structurally and dielectrically almost identical alkoxy biphenyl M in Table 2 shows a surprisingly large difference of almost a factor of 4 between the rotational viscosities. The discrepancy between the different values of γ_1 and the almost identical molecular basic structures of K and M makes it difficult to envisage a qualitative explanation for this finding based on specific molecular properties. However, it may be that molecular resonance phenomena lead to remarkable differences of the average molecular structure in alkoxy type cyano biphenyls M compared with the non-mesomeric alkyl biphenyls K. Due to the electron-donating oxygen in the alkoxy chain of Ms the following resonance structure is likely to occur;

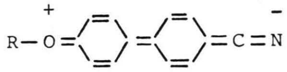

The availability of this planar resonance structure may favour bimolecular associates which may in turn lead to higher γ_1-values. On the other hand such enhanced pairing is also expected ro raise the clearing temperature which would be in agreement with the higher T_c-values of M_s compared with Ks.

The average shear viscosity η_s is not a very transparent quantity. With regard to applications it is nevertheless interesting to look at correlations between the ratio γ_1/η_s and molecular structural properties. Large ratios around $\gamma_1/\eta_s = 6$ were found for mixtures comprising hydrogenated components such as PC, EC and PE (Table 1). The molecules with two benzene rings were found to exhibit values from 4 to 5, whereas PD and MBBA show low ratios of ~ 3 (Table 1).

With respect to the temperature dependence of γ_1, characterized roughly by T_{a,γ_1}, one can distinguish three more or less distinct groups of binaries among these depicted in Table 1. The highest values of T_{a,γ_1} — well above 6 kK — were found for MBBA and the cyanoesters E. The second group consists of the directly connected two-ring molecules M, P, PD and K as well as of the cyano Schiff'base S. This group shows values of T_{a,γ_1} ranging from 5.3 to 5.7. The lowest values were found for the hydrogenated binaries PC, PE and EC (Table 1). Among the latter the hydrogenated esters EC and PE exhibit particularly low values of $T_{a,\gamma_1} \approx 4.4$ kK while $T_{a,\gamma_1} = 4.9$ kK of the phenyl cyclohexanes is somewhat higher. It is perhaps tempting to seek the reason for such low T_a-values in the flexibility of the molecular shape which is to some extent given by the many possible conformations of the cyclohexane ring. This tentative explanation assumes, however, an unproved relation between molecular flexibility and activation energy. However, most noticeable is the fact that low values of T_{a,γ_1} seem to correlate well with high values of γ_1/η_s.

The rotational viscosities of mixtures (P7, X) comprising — besides P7 — components of different substance classes (Table 2) show interesting nonlinear effects. Only for the mixture comprising PD was a reduction of γ_1 found which would about correspond to a straightforward interpolation between γ_1(P) and γ_1(PD), whereas mixtures (P, X), where X = PC and EC respectively, exhibit disproportionally large viscosity reductions. On the other hand the addition of MBBA to P7 leads to a smaller reduction than expected. The temperature dependence of mixtures (P, X) in Table 2 is in all cases stronger (higher $T_{a,\gamma}$) than one would expect from considering the activation energies of the respective basic mixtures in Table 1. In all cases — expect for (P, EC) — a pronounced increase of T_{a,γ_1} is observed in mixtures (P, X). For (P, EC) the reduction of T_{a,γ_1} is very small although Table 1 would suggest a drastic reduction. Thus, mixing different classes of substances leads in our cases to a relatively strong temperature dependence of γ_1.

4. Electro-optical Response in Twisted-nematic Cells

The response of the transmission of twist cells to sudden changes of applied voltages was measured using two different driving schemes. First the response to small voltage changes was determined. This allows a quantitative comparison of the measured response times with those determined from approximate calculations of the dynamic behaviour of twist cells [9]. Besides, the response behaviour of twist cells upon application of rather high gated voltages was measured and compared in a more heuristic manner with LC-material parameters.

4.1. Small Scale Relaxation

Multiplexed twist cells are addressed so that the applied difference between the select voltage and the nonselect voltage is as small as possible but still large enough to produce large transmission changes. The voltage at the non-select display elements is chosen below that of the optical threshold. Owing to the transmission characteristics of twist cells the corresponding changes of the director pattern are relatively modest. To characterize the dynamics of small voltage changes we have performed measurements by switching the applied voltage in either direction between the values corresponding to the respective transmissions of 37% and 63% of twist cells. Monochromatic light of $\lambda = 546$ nm was used. The average of the two relaxation rates as determined from the two response measurements was taken to be representative for the slowest small-scale relaxation processes corresponding with the director deformation at the 50%-transmission voltage. Table 3 contains these measured relaxation times t_{50} of mixtures 1 to 8 together with the temperatures T_m at which the measurements were made.

To compare the measured response times t_{50} with the viscosity data we have listed in Table 3 the characteristic times [10]

$$\tau_0 = \gamma_1 d^2 / k_{22} \pi^2 , \tag{4.1}$$

where k_{22} is the twist elastic constant. The time τ_0 sets the basic scale on which the dynamic phenomena take place [9]. Also shown in units of τ_0^{-1} are the calculated rates r_θ and r_φ. These rates belong

Table 3. Electro-optical response of 10 μm spaced twist cells for small changes of driving voltage. The response times t_{50} were measured at the temperatures T_m. The voltage was switched in both directions between values corresponding to 37% and 63% transmission; t_{50} is the average of the two values. Also shown are values for τ_0 (4.1) and calculated response rates r_θ and r_φ in units of τ_0^{-1}.

	T_m [°C]	t_{50} [ms]	τ_0 [ms]	r_θ	r_φ	$\frac{t_{50}}{\tau_0} \frac{r_\theta + r_\varphi}{2}$
E	30	109.9	560	4.44	4.38	0.865
S	30	87.8	527	4.97	4.78	0.812
K	20	76.4	311	3.91	3.91	0.961
M	30	103.0	537	3.91	3.93	0.752
PE	45	45.3	246	3.88	3.66	0.694
PC	20	61.2	318	4.51	4.20	0.838
PD	35	66.0	190	2.74	2.84	0.969
P	30	66.1	278	3.12	3.25	0.757

to the two slowest small scale processes that restore the deformation pattern of the nematic director towards the one corresponding to an applied voltage V_{50}. The rates r_θ and r_φ follow from numerical calculations which treat the dynamics of the twisted structure in an approximation neglecting mass flow [9]. In this treatment γ_1 is the only viscosity coefficient determining the dynamics of the cell. The rates r_θ and r_φ are characteristic for the state of the deformation of the twisted structure. They depend on the elastic constant ratios and on the dielectric anisotropy. Values for these parameters were taken from [6]. For the actual deformations in our systems r_θ and r_φ are almost equal for a given substance. Thus, the average of r_θ and r_φ was taken for comparing the calculated rates with the experimentally determined relaxation times t_{50}. The last column of Table 3 shows the ratio of the measured relaxation times t_{50}/τ_0 and the calculated relaxation times $2/(r_\theta + r_\varphi)$. These ratios show an average of 0.83 with a scatter of 0.10. Some of this scatter can be attributed to experimental uncertainties but it is likely that some of it as well as the systematic deviation of these ratios from 1 (Table 3) originate from neglecting backflow effects in the theoretical treatment. Nevertheless, the results show that the viscosity coefficient γ_1, together with the elastic and dielectric parameters, characterizes the small-scale dynamics of a twisted nematic cell for all LC classes investigated rather well.

4.2. Dynamics of Large Deformation Changes

The second set of experiment was made by switching the applied cell voltage between zero and a value V_{on} corresponding to 2.5 times the 10%-transmission voltage (100% transmission at high voltages). From these experiments two characteristic turn-on times have been measured, namely t_{on} (10%) which is the time required for the transmission to reach 10% of its full value, as well as $\Delta t_{\text{on}} = t_{\text{on}}(50\%) - t_{\text{on}}(10\%)$ which is the time required for the transmission to increase from 10% to 50%. The measured turn-off time t_{off} is the time required for the transmission to decay from 100% to 10%. It must be emphasized that especially the turn-off transmission shows rather pronounced "bouncing"; therefore, t_{off} is only a crude characterization of the turn-off dynamics, though it is important from an application point of view. The values of $t_{\text{on}}(10\%)$, Δt_{on} and t_{off} measured 10 °C below the clearing temperature are shown in Table 4. For the rise- and decay times Jakeman and Raynes [10] have proposed heuristic expressions of the form

$$\tau_{\text{decay}} = \frac{\eta d^2}{k \pi^2},$$

$$\tau_{\text{rise}} = \frac{\eta d^2}{k \pi^2} / [(V/V_{\text{c}})^2] - 1, \tag{4.2}$$

in which η is a representative viscosity, most suitably γ_1, and k is the combination of elastic constants $(k_{11} + \frac{1}{4} k_{33} - \frac{1}{2} k_{22})$ which determines the threshold voltage V_{c} for the director deformation of the twisted structure. The aim of comparing these expressions (which hold for small angles of deformation only) with measured response times is to find empiric correlations rather than to expect a detailed understanding of the switching processes. Table 4 shows ratios of measured response times and the values obtained by inserting the respective material parameters from [6] into (4.2). The values of $t_{\text{off}}/\tau_{\text{decay}}$ and of $t_{\text{on}}/\tau_{\text{rise}}$ show a considerably narrow scatter of ±15% which is a rather satisfactory correlation. On the average the ratio $t_{\text{off}}/\tau_{\text{decay}}$ has a value of 0.58 (Table 4). That this value lies below one may have various reasons such as (i) the inadequacy of applying the small angle deformation expression (4.2) to the large scale deformations taking place upon switching the applied voltage off or (ii) the extremely nonlinear change of transmission with changing deformation. However, more important than accurate absolute estimates for t_{off} is a correct representation of the trends which are quite accurately given by τ_{decay}. The values of $t_{\text{on}}/\tau_{\text{rise}}$ are centered around 5.9. This large value can possibly be explained by the initially labil equilibrium of the zero-voltage twist structure at the time a field is applied. There have been attempts to describe the turn-on behaviour of twist cells by distinguishing between a delay time and a rise time. The delay time, for which our t_{on} may be representative, characterizes the first step in the turn-on process during which the long axes of the molecules in the helical structure, attempt so to say to find their way out of the planar off-state. Thus, the time $\Delta t_{\text{on}} = t_{\text{on}}$ (50% transmission) $- t_{\text{on}}$ (10% transmission), during which the initial labil equilibrium no longer exists, is a more adequate response parameter than t_{on} to describe the dynamics towards the on-

Table 4. γ_1 and electro-optical response of 10 μm spaced twist cells using gated driving voltages and measured 10 °C below the respective clearing temperatures of the mixtures. The driving voltage V_{on} was 2.5 times the voltage required to achieve 10% transmission. The ratios $V_{\text{on}}/V_{\text{c}}$ as well as τ_{decay} and τ_{rise} were calculated from (4.2) using γ_1 and the material parameters of [6].

	t_{on} (10%) [ms]	$\triangle t_{\text{on}}$ [ms]	t_{off} [ms]	$\frac{V_{\text{on}}}{V_{\text{c}}}$	$\frac{t_{\text{off}}}{\tau_{\text{decay}}}$	$\frac{t_{\text{on}}(10\%)}{\tau_{\text{rise}}}$	$\frac{\Delta t_{\text{on}}}{\tau_{\text{rise}}}$	γ_1 [Poise]
E	52.4	9.0	70.4	4.07	0.476	5.52	0.948	0.96
S	31.3	6.4	38.8	3.82	0.542	5.95	1.216	0.50
K	56.4	—	69.4	3.89	0.641	7.36	—	0.76
M	35.4	7.8	42.9	3.73	0.569	6.06	1.335	0.40
PE	24.0	4.1	28.5	3.46	0.455	4.20	0.718	0.37
PC	25.3	7.3	34.4	3.73	0.682	6.48	1.870	0.39
PD	48.9	8.4	66.2	3.56	0.674	5.81	0.999	0.51
P	42.6	6.9	61.4	3.90	0.586	5.78	0.936	0.74

state. Measurements of Δt_{on} which are compared with τ_{rise} are shown in Table 4. The average of the ratios $\Delta t_{\text{on}}/\tau_{\text{rise}}$ turned out to be 1.15, scattering by ±33%. Thus, although τ_{rise} gives a much more accurate absolute value for Δt_{on} than for t_{on} its predictive power is larger for t_{on} than for Δt_{on}. Correlations of this type have been looked for previously, however, in these attempts the shear viscosity η_{s} was used instead of γ_1 [8, 11, 12].

5. Conclusions

We have measured the temperature dependence of the rotational and shear viscosities γ_1 and η_{s} of binary mixtures belonging to ten structurally markedly different liquid crystal classes. An attempt was made to relate γ_1 qualitatively with molecular properties. Besides, we have investigated the dynamics of twisted nematic cells under different driving conditions and related the electro-optical response with the respective elastic, dielectric and rotational viscosity material constants. For the small-scale dynamics of twist cells good agreement was found for all liquid crystal materials between calculated and measured response behaviour. This result shows that γ_1 is indeed the crucial viscosity determining the dynamics of twist cells.

From measurements of the rotational viscosity γ_1 and comparisons with η_{s} we found for all liquid crystal classes and temperatures $3 < \gamma_1/\eta_{\text{s}} < 7$. Thus, the viscosity ratios γ_1/η_{s} were found not to be constant but to vary by more than a factor of 2 among different materials. Our results indicate that strongly positive dielectric nematics exhibit considerably larger γ_1-values than structurally similar non-polar molecules. Hydrogenation of one aromatic ring in liquid crystals comprising two rings was found — contrary to the effect on η_{s} — to hardly affect γ_1. However, our results show that the activation energy of $\gamma_1(T)$ of hydrogenated compounds and therefore also the temperature dependence of γ_1 decreases compared with aromatic counterparts. γ_1 of the dielectrically and structurally very similar cyano alkyl and alkoxy biphenyls were found to differ by almost a factor of 4. This surprising result may be due to the occurrence of molecular resonance structures in cyano alkoxy biphenyls leading to planar structures which may enhance the affinity towards molecular pairing.

Acknowledgement

We thank U. Witschi and B. Blöchliger for their assistance in the experimental work.

[1] Ch. Gähwiller, Mol. Cryst. Liq. Cryst. **20**, 301 (1973).
[2] K. Skarp, S. T. Lagerwall, and B. Stebler, Mol. Cryst. Liq. Cryst. **60**, 215 (1980).
[3] H. Kneppe, F. Schneider, and N. K. Sharma, to be published.
[4] K. Zvetkov, Acta Phys. URSS **18**, 358 (1943).
[5] G. Heppke and F. Schneider, Z. Naturforsch **27a**, 976 (1972).
[6] M. Schadt and P. R. Gerber, Preceeding Paper.
[7] P. R. Gerber, Appl. Phys. **A26**, 139 (1981).
[8] M. Schadt and F. Müller, Rev. Phys. Appl. **14**, 265 (1979).
[9] P. R. Gerber, Appl. Phys. **25**, 259 (1981).
[10] E. Jakeman and E. P. Raynes, Phys. Lett. **A39**, 69 (1972).
[11] M. Schadt and F. Müller, IEEE Trans. Electron Devices **ED25**, 1125 (1978).
[12] J. Constant and E. P. Raynes, Mol. Cryst. Liq. Cryst. **62**, 115 (1980).